Towards Reduced Order Modelling of Cardiac Electroanatomical Mapping

Olivier Crabbé[1,2], Karim El Houari[2], Louis Rigal[1], Sophie Collin[2], Pierre L'Eplattenier[2], Christelle Grivot[2], Michel Rochette[2], Antoine Simon[1], Pascal Haigron[1], Raphaël Martins[1]

[1] Univ Rennes, CHU Rennes, LTSI, Inserm - U1099, Rennes, France
[2] Ansys Inc., Canonsburg, PA, USA

Abstract

Ventricular tachycardia (VT) is a lethal heart rhythm disorder responsible for 80% of sudden cardiac deaths. Radiofrequency ablation (RFA) of VT is minimally invasive and potentially curative but target identification using cardiac electroanatomical mapping (EAM) is challenging. Personalized computer heart models may provide deeper insight of patient electrophysiology (EP) but are often incompatible with clinical timeframes.

This work is a proof of concept of applying personalized finite element EP modeling and machine learning (ML) to achieve near-instant prediction of patient EAM in sinus rhythm. We used one patient dataset to generate a personalized 3D left-ventricle model. A simulation batch with varying parameters was run and results were compared to patient EAMs. Simulated data was then used to generate a reduced order model (ROM) through ML. ROMs were capable of reproducing the simulation activation maps with $< 1\,\mathrm{ms}$ *accuracy using as low as 15 learning scenarios.*

1. Introduction

Cardiac arrhythmia is a major cause of sudden cardiac death (SCD), representing over 10% of worldwide all-cause mortality. Among cardiac arrhythmias, ventricular tachycardia (VT) is responsible for 80% of SCDs [1]. Most ventricular arrhythmias are linked to structural cardiopathy, following myocardial infarction (MI) or congenital heart disease repair.

A potentially curative treatment of structural VT is radio frequency ablation (RFA) of the arrhythmic substrate via catheterization. The RFA involves identification followed by ablation of the critical VT isthmus, usually located in the scar boundary zone (BZ). However, the challenges of isthmus identification combined with the lack of consensus on ablation strategies leads to a 25 to 50% recurrence rate [1], making this treatment option sub-optimal.

Patient-specific computer models of heart electrophysiology (EP) can be a useful tool to assist the clinicians during RFA by providing a full electrical activation map of the ventricles. Our challenge is producing accurate personalized simulation models, particularly with regards to tissue electrical properties. As the *in-vivo* measurement of such quantities is difficult, calibration of the virtual-heart parameters through simulation result comparison to measured 12 lead electrocardiograms (ECGs) and electroanatomical maps (EAMs) is proving to be an interesting alternative [2–8]. However, to reliably achieve parameter calibration, a great number of simulations is needed, which is incompatible with the simulation time of state-of-the-art reaction-diffusion models.

Machine learning (ML) has been identified as an option to reduce simulation time. Several successful attempts at metamodel creation have been made using regressions [2, 5], variational auto-encoders [4] and polynomial chaos spectral approximation [6]. This study presents a simple data-driven approach to generate a reduced order model (ROM) capable of rapidly computing the endocardium activation time field for a given parameter set. In the following sections, we describe the patient dataset, the patient-specific finite-element left-ventricle EP model used for data generation, the ML algorithm applied on said data and the corresponding simulation and ROM results.

2. Materials and Methods

2.1. Clinical Data

Subject was a 50-year-old male patient referred for RFA procedure targeting LV endocardial VT linked to a large MI located in the postero-apical portion of the LV. The patient's dataset includes clinical cardiac delayed enhanced magnetic resonance imaging (DE-MRI), clinical cardiac Cine MRI, clinical high-resolution computed tomography (CT), CARTO3 (Biosense Webster - Irvine, CA, USA) system EAMs and 12-lead ECG signals, both recorded during the RFA procedure in sinus rhythm and pacing-induced VT. Both MRI sequences were acquired one year prior to the rest of the data. Subject underwent implantable cardioverter-defibrillator (ICD) implantation during said 1-year gap, resulting in a large artifact in the preoperative CT.

The available DE-MRI, Cine-MRI and CT had $0.9 \times 0.9 \times 12\,\mathrm{mm}$, $1 \times 1 \times 10.5\,\mathrm{mm}$ and $0.6 \times 0.6 \times 0.7\,\mathrm{mm}$ voxels respectively. The sinus rhythm EAM contained an endocardium mesh and the latency values for 1144 annotation points after outlier removal.

2.2. 3D Patient-Specific LV Model

2.2.1. Patient-Specific LV Geometry

Patient-specific geometry was reconstructed from cardiac CT imaging. Segmentation was done manually using MITK [9] as the ICD artifact made automatic segmentation challenging. A 3D-surface mesh was then reconstructed and smoothed using 3D-Slicer [10] and shrinkwrapped using Ansys SpaceClaim (Ansys Inc. - Canonsburg, PA, USA) with a target triangle size of $1\,\mathrm{mm}$. Volume meshing was done based on the resulting triangulated surface using Gmsh [11] to obtain a tetrahedral simulation mesh composed of ~ 300 thousand nodes.

2.2.2. Anatomical Features

Tissue labels were deduced from DE-MRI signal intensity (SI). LV myocardium (MC) was manually segmented using 3D-Slicer. MC voxel labels were then deduced from SI using the standard deviation method described in [12]. In short, the mean and standard deviation of SI in remote healthy MC is computed and thresholding is applied based on the obtained values. Label transfer from MRI to CT was done using the in-house tool CRTPlanning [13].

Purkinje network and fiber orientation were both computed using pyheart-lib [14] and LS-DYNA (Ansys Inc. - Canonsburg, PA, USA). Fiber orientation was computed for each element in the tetrahedral mesh using a commonly used rule-based approach described in [15]. The Purkinje network was modelled as a fractal beam network originating from the LV endocardium apex using a method described in [16]. The impulse onset location was set at the origin of the Purkinje network.

2.3. Electrophysiological Modelling

Healthy MC was modelled using the ten Tusscher-Noble-Noble-Panvilov (TNNP) model [17]. Transmural heterogeneity was modelled by differentiating subendocardial, M-cell and epicardial regions, spanning respectively 17, 41 and 42% of the ventricular wall thickness as done in [18]. Macroscopic diffusion was modelled using the monodomain model [19]. The fiber direction macroscopic conductivity σ_f was set to $0.5\,\mathrm{S\,m^{-1}}$ in healthy tissue.

Electrical remodelling in the BZ was introduced in both macroscopic and cellular scales. The TNNP model maximum conductances I_{Kr}, I_{Ks}, I_{Na} and I_{CaL} were reduced to 30, 20, 38 and 31% of their original values respectively, as done in [18,20]. The fiber and cross-fiber direction conductivities (σ_f and σ_t) in the BZ were also reduced to 20% of the values used for the healthy MC. Scar tissue was considered as non-conductive.

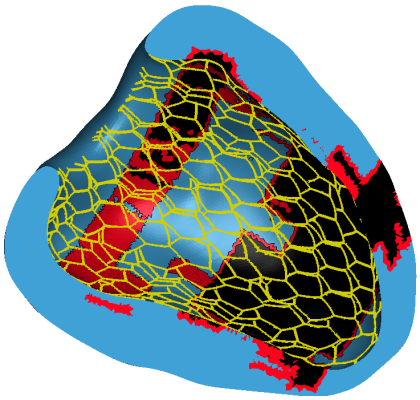

Figure 1. Section view of the LV model. Blue: Healthy MC. Red: BZ. Black: Scar. Yellow: Purkinje Network.

The Purkinje network's conductivity σ_p is set to 6 times the healthy fiber direction conductivity. Impulse initiation is achieved by forcing the transmembrane potential value to $50\,\mathrm{mV}$ for $5\,\mathrm{ms}$ on the chosen onset nodes.

2.4. Data-driven Machine Learning

2.4.1. Data Generation

The data generated for the ML application comprised 150 scenarios with varying model parameters. The varying parameters chosen in this study were the MC anisotropy ratio (σ_t/σ_f) and the cell surface-to-volume ratio (β), the respective ranges being $[0.1; 0.8]$ and $[75; 200]\,\mathrm{mm^{-1}}$.

The monodomain and cellular model equations were solved in LS-DYNA using backward and forward Euler schemes respectively. The time step for both numerical solutions was set to $0.05\,\mathrm{ms}$. Single-heartbeat simulations of $1000\,\mathrm{ms}$ simulated time had a computation time of approximately ten minutes using a parallel computing system of 320 processors.

2.4.2. Reduced Order Model Construction

The ROM construction was performed using the Static ROM Builder tool in Ansys Twin Builder (Ansys Inc. - Canonsburg, PA, USA). The chosen approach relies on data reduction followed by interpolation to generate a ROM capable of near-instantly approximating the endocardial activation time field for any given (β , σ_t/σ_f) pair. The ROMs are generated with a set of learning scenarios (LS) and their performance is assessed by comparing ROM estimations to a set of validation scenarios (VS).

More precisely, once the simulations were run, the activation time values were exported from all non-scar nodes in the endocardium for each simulated scenario. Among the 150 scenarios, 26 were discarded for having unrealistic conduction velocities. Among the rest, 24 were chosen as VS and 100 as the learning set. Three ROMs were created using 15, 40 and 100 LS out of the learning set.

Data reduction was achieved through Singular Value Decompostion (SVD), allowing for the endocardial activation time fields to be approximated by a linear combination of a handful of orthogonal vectors called SVD modes. Once the modes and the mode coefficients for each LS were deduced, interpolation of said coefficients was achieved using the GARS algorithm [21].

2.5. Validation

Result validation in this study was done in two steps. First, the original simulation results were compared to the EAM ground-truth data to check overall accuracy of the model. Activation time information was transferred from the EAMs to the simulation mesh endocardium through semi-automatic registration of the two meshes using the CardioMerge software [22] followed by a projection of the annotation points onto the closest simulation mesh node. A distance-weighted average was applied in case of overlap.

The second step, independent of the first, was done to assess fidelity of the ROMs with respect to the LV monodomain model on which they are based.

3. Results

3.1. EAM Comparison

After projection of the 1144 CARTO3 points onto the simulation mesh endocardium, with an average projection distance of $9.4\,\mathrm{mm}$, all the simulated scenarios were compared to the ground truth data. The minimum and maximum mean errors across scenarios were $29\,\mathrm{ms}$ and $36\,\mathrm{ms}$ respectively, the maximum error in both corresponding scenarios being $56\,\mathrm{ms}$.

3.2. ROM performance

ROM errors are summarized in Table 1. ROMs estimated each activation time field in less than one second. As one could expect, both the mean and maximum errors in ROM estimations decreased as the LS number increased. As computational cost of the data generation phase increases linearly with the amount of learning data, smaller LS numbers are preferred and still allow for acceptable mean errors. Figure 2 depicts the maximum errors in the 15 LS ROM estimations across the tested parameter sets. Regarding maximum error, the highest values appeared in low conduction velocity scenarios (high β , low σ_t/σ_f). In these cases, late activation sites formed locally in the BZ, likely due to numerical error in the simulations. The ROMs could not correctly capture this local behavior as it was sub-represented in the learning set. However, this only resulted in 3.6% of non-scar endocardium nodes having errors above $1\,\mathrm{ms}$ across all estimations made by the 15 LS ROM. Higher LS numbers do not significantly reduce the value of these local errors but do decrease the amount of points with error above $1\,\mathrm{ms}$.

Table 1. ROM error summary. Mean activation time (excl. scar) varies between 50 and $77\,\mathrm{ms}$ across scenarios.

LS nb.	Mean error	Max. error	$\% > 1\,\mathrm{ms}$*
15	$0.10\,\mathrm{ms}$	$56\,\mathrm{ms}$	3.6%
40	$0.05\,\mathrm{ms}$	$48\,\mathrm{ms}$	1.8%
100	$0.04\,\mathrm{ms}$	$55\,\mathrm{ms}$	1.8%

*% of non-scar nodes having max ROM errors above $1\,\mathrm{ms}$.

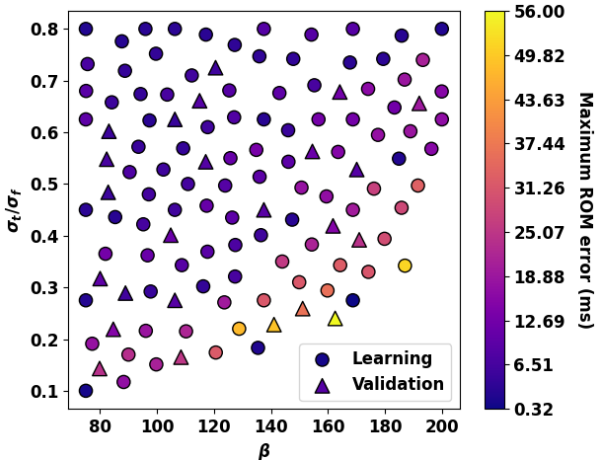

Figure 2. Maximum errors in the 15 LS ROM estimations across parameter sets.

4. Discussion

In this study, a proof-of-concept application of simple model reduction techniques to personalized heart EP simulation was demonstrated. The ROMs presented reproduced simulation results accurately with a significant reduction in computation time using as low as 15 LS.

The limitations of our study are mostly linked to the simulation model. A major flaw in this model is quite obviously the tissue label information acquisition. Not only is the resolution of the DE-MRI limited, the image stack was also obtained a year prior to the RFA intervention, possibly shortly after the patient's MI when the affected tissue would be under a transient state of significant inflammation and remodelling [23]. To add to the labelling imprecision, the standard-deviation thresholding is used without an assessment of its uncertainty. Labelling imprecision

contributes $22.3\,\mathrm{ms}$ to the mean simulation errors, as 66% of EAM points are matched to scar nodes on our mesh.

Another limitation of our model is the information transfer between different data sources. Label transfer from DE-MRI to the CT was based on a rigid registration that had to compromise between LV MC overlap and LV endocardium apex correspondence, further increasing tissue label uncertainty. The registration and projection of the EAM data onto the simulation mesh is also a major candidate for further study as result validation and future parameter personalization will heavily depend on it.

Lastly, there was no attempt at personalizing the Purkinje network origin, shape or conductivity. This step is to be included in future work, using a similar approach to [3], as the Purkinje network was observed to be the prime influencer of endocardial activation times in our model.

Although a better match of the original model to the EAM data is yet to be achieved, it still contains key anatomical features that the ML algorithm is capable of handling. With that in mind, we can argue that the presented algorithm should have similar performance on more accurate models of the same or other patients, provided they contain similar features. This ability to construct reliable, real-time heart EP simulators for a few given parameters is an important step toward real-time EP parameter personalization based on EAM data.

References

[1] Dukkipati et al. Catheter Ablation of Ventricular Tachycardia in Structural Heart Disease: Indications, Strategies, and Outcomes—Part II. *Journal of the American College of Cardiology*, 70(23):2924–2941, December 2017.

[2] Zettinig et al. Data-driven estimation of cardiac electrical diffusivity from 12-lead ECG signals. *Med Image Anal*, 18(8):1361–1376, December 2014.

[3] Gillette et al. Automated Framework for the Inclusion of a His–Purkinje System in Cardiac Digital Twins of Ventricular Electrophysiology. *Ann Biomed Eng*, 49(12):3143–3153, December 2021.

[4] Dhamala et al. Embedding high-dimensional Bayesian optimization via generative modeling: Parameter personalization of cardiac electrophysiological models. *Medical Image Analysis*, 62:101670, May 2020.

[5] Giffard-Roisin et al. Noninvasive Personalization of a Cardiac Electrophysiology Model From Body Surface Potential Mapping. *IEEE Trans Biomed Eng*, 64(9):2206–2218, September 2017.

[6] Konukoglu et al. Efficient probabilistic model personalization integrating uncertainty on data and parameters: Application to eikonal-diffusion models in cardiac electrophysiology. *Prog Biophys Mol Biol*, 107(1):134–146, October 2011.

[7] Relan et al. Coupled personalization of cardiac electrophysiology models for prediction of ischaemic ventricular tachycardia. *Interface Focus*, 1(3):396–407, June 2011.

[8] Wallman et al. Computational methods to reduce uncertainty in the estimation of cardiac conduction properties from electroanatomical recordings. *Medical Image Analysis*, 18(1):228–240, January 2014.

[9] Wolf et al. The medical imaging interaction toolkit. *Med Image Anal*, 9(6):594–604, December 2005.

[10] Fedorov et al. 3D Slicer as an Image Computing Platform for the Quantitative Imaging Network. *Magn Reson Imaging*, 30(9):1323–1341, November 2012.

[11] Christophe Geuzaine and Jean-François Remacle. Gmsh: A 3-D finite element mesh generator with built-in pre- and post-processing facilities. *International Journal for Numerical Methods in Engineering*, 79(11):1309–1331, 2009.

[12] Kim et al. Relationship of MRI Delayed Contrast Enhancement to Irreversible Injury, Infarct Age, and Contractile Function. *Circulation*, 100(19):1992–2002, November 1999.

[13] Nicolas Courtial. *Fusion d'images multimodales pour l'assistance de procédures d'électrophysiologie cardiaque*. PhD thesis, March 2020.

[14] Hoeijmakers et al. pyheart-lib: A Python Library for LS-DYNA Multi-physics Heart Simulations. In *Functional Imaging and Modeling of the Heart*, pages 565–574, 2023.

[15] Bayer et al. A Novel Rule-Based Algorithm for Assigning Myocardial Fiber Orientation to Computational Heart Models. *Ann Biomed Eng*, 40(10):2243–2254, October 2012.

[16] Sahli Costabal et al. Generating Purkinje networks in the human heart. *Journal of Biomechanics*, 49(12):2455–2465, August 2016.

[17] K. H. W. J. ten Tusscher and A. V. Panfilov. Alternans and spiral breakup in a human ventricular tissue model. *American Journal of Physiology-Heart and Circulatory Physiology*, 291(3):H1088–H1100, September 2006.

[18] Lopez-Perez et al. Personalized Cardiac Computational Models: From Clinical Data to Simulation of Infarct-Related Ventricular Tachycardia. *Frontiers in Physiology*, 10, 2019.

[19] Bradley J. Roth. The electrical potential produced by a strand of cardiac muscle: A bidomain analysis. *Ann Biomed Eng*, 16(6):609–637, November 1988.

[20] Arevalo et al. Arrhythmia risk stratification of patients after myocardial infarction using personalized heart models. *Nat Commun*, 7:11437, May 2016.

[21] Malek Ben Salem and Lionel Tomaso. Automatic selection for general surrogate models. *Structural and Multidisciplinary Optimization*, February 2018.

[22] Rigal et al. Multimodal fusion workflow for target delineation in cardiac radioablation of ventricular tachycardia. *Medical Physics*, 51(1):292–305, 2024.

[23] Romito et al. In vivo assessment of regional mechanics post-myocardial infarction: A focus on the road ahead. *J Appl Physiol (1985)*, 123(4):728–745, October 2017.

Address for correspondence:

Olivier Crabbé

Ansys France

35-37 Rue Louis Guérin - 69100 Villeurbanne, France

olivier.crabbe@etudiant.univ-rennes.fr